

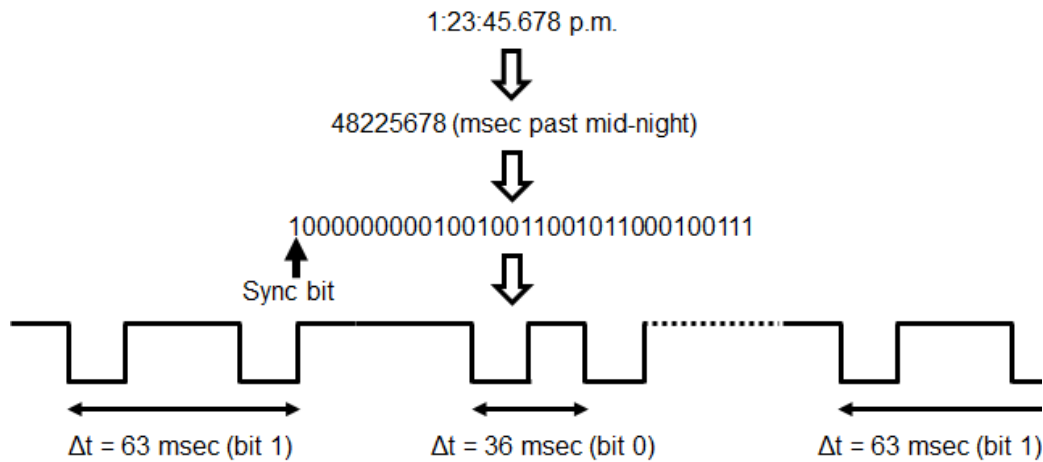
SUPPLEMENTAL DATA

Improving the temporal resolution of the externally tracked motion data

A time injection algorithm was developed that encodes the absolute Vicra host PC system time and injects it into the PET list-mode data stream via one scanner physiological gating input. Logically, this time information is in the form of a sync bit followed by 32 bits of an unsigned integer representing the millisecond past mid-night at which the leading edge of the sync pulse arrived. Physically, this is accomplished by strategically driving the Vicra host PC RS-232 serial port as a waveform generator, which is connected to a scanner gating input through an RS-232 to TTL level converter (B&B Electronics 232LPTTL). The scanner responds to the falling edge of a TTL signal by inserting a gating data packet into the list-mode stream. With the serial port configured for a baud rate of 110 bps, transmitting the 8-bit ASCII character 0x3E results in a pair of falling edges 36.36 milliseconds apart (a 0 bit). Similarly, transmitting 0x06 yields a pair of falling edges 63.63 milliseconds apart (a 1 bit). In either case, the scanner will insert a pair of gating data tags. List-mode parsing software can distinguish these two cases because scanner gating inputs are sampled every millisecond and time tags are inserted every millisecond. A delay of 200 milliseconds between successive virtual bit transmissions guarantees separation between these gating tag pairs. A delay of 5 seconds provides separation between successive time insertions. Thus, each absolute time injection requires 66 falling edges at the scanner gating input, since there are 33 bits (sync bit plus 32 data bits). The least significant bit of the time is transmitted first.

The PET list-mode data file is pre-processed before reconstruction to decode the absolute times of the sync pulses, which are matched to their nearest list-mode time tags in order to calculate the absolute times of all time tags in the list-mode file, and thus to synchronize the PET list-mode data and the motion data. One time synchronization packet is injected to the list-mode

stream approximately every 10 seconds, and the time stamps in the list-mode data are synchronized with the motion data whenever a new time synchronization packet is received, which accounts for possible inconsistency in the system clock speed between the PET scanner and the Vicra motion tracking system. For a 30-min scan, the offsets typically drift by a few msec, due to such inconsistencies. An example of the time synchronization technique is shown in Supplemental Fig. 1.

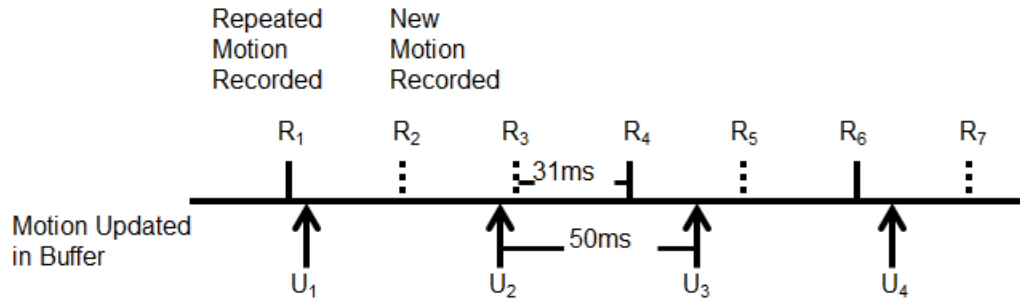


Supplemental Fig. 1. Example of the time synchronization algorithm. The absolute time (in msec) past midnight is converted to an integer, which is represented in binary format. The bits are coded by two gating pulses separated by 36 or 63 msec for bit 0 or bit 1, respectively.

The above time synchronization method can reduce the temporal uncertainty in the motion data to <50 msec. This uncertainty is due to the combined effects of 1) the time taken to acquire and calculate motion data by the Vicra system (estimated at ~ 17 msec, based on the highest operating rate of 60 Hz and 2) the difference between the time when motion data are stored in the Vicra system buffer and the time when motion data are read from the buffer and recorded to a motion data file. This buffer is updated every 50 msec, since the acquisition rate is 20 Hz. The host PC polls this buffer (asynchronously) every 31 msec and writes the read out tracking data to

disk file, along with a time stamp which defines the time when motion data are read from the buffer (not the time when the camera images were acquired). The second effect can be eliminated by the following algorithm.

We make use of the fact that motion data are *recorded* to file every 31 msec, whereas new motion data are *updated* in the buffer approximately every 50 msec. Therefore, pairs of identical position values are found in the motion file if two 31-msec reads fall into one 50-msec update interval. Assuming that motion data are updated in the buffer at equal time intervals that are very close to 50 msec, we were able to use the information from the repeated motion data to determine when motion data are updated in the buffer, as elaborated in Supplemental Fig. 2. Specifically, time points R_1 to R_7 denote when motion data are recorded to a motion file, and time points U_1 to U_4 denote when new motion data are updated in the motion data buffer in the Vicra system. In the example in Supplemental Fig. 2, R_3 and R_4 have the same motion data since no new motion data were available between R_3 and R_4 , but R_4 and R_5 have different motion data since new motion data became available at time point U_3 . Therefore, using the information of the time points when repeated and new motion data are written to the motion file, and assuming that the motion data buffer is updated approximately every 50 msec, we estimated the buffer update times U_i . This estimation was performed iteratively with the constraint that U_i values remain consistent with the repeat pattern in the R values. The optimization criterion was the minimization of the standard deviation of the time interval between U_i values (ΔU_i). Typically, ΔU_i converged to 50.0 ± 1.3 msec.



Supplemental Fig. 2. Determining the actual time when motion data are updated in the buffer from the recorded motion data. Time points R_1 to R_7 denote when motion data are written to a motion file, and time points U_1 to U_4 denote when new motion data are updated in the motion data buffer in the Vicra system. The dashed lines (R_2 , R_3 , R_5 and R_7) represent the times when new motion data are written to the motion data file, and the solid lines (R_1 , R_4 and R_6) represent when repeated motion data are written. In this example, R_3 and R_4 have the same motion data since there were no updates between R_3 and R_4 in the motion data buffer, but R_4 and R_5 have different motion data an update occurred at time point U_3 in the motion data buffer. Therefore, using the information of the time points when repeated and new motion data are written to the motion file, and assuming that the motion data buffer is updated every 50 msec, the exact time points U when the motion data are updated in the buffer can be estimated.

Evaluation of the time synchronization technique using a moving rod source scan

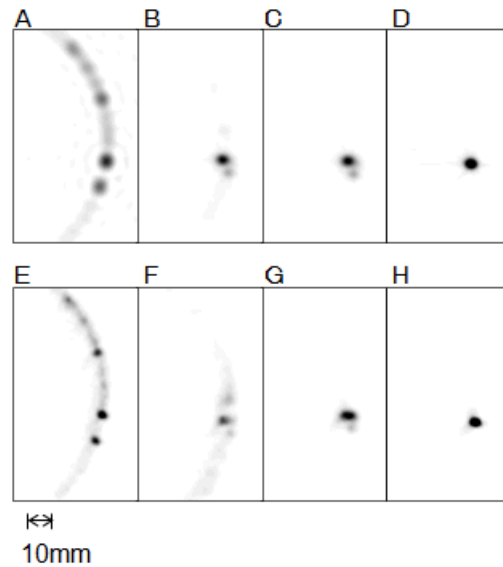
To validate the time synchronization technique, a ^{68}Ge rod source (30 MBq, Sanders Medical) was placed along the axial direction of the scanner FOV. A 2-min static scan was acquired, followed by a 2-min dynamic scan, in which the rod source was manually rotated along a circular track bounded by the scanner transaxial FOV. Reflective markers were attached to the end of the rod source and motion data were recorded by the Vicra system. The time synchronization package was used to send the system time of the Vicra PC to the PET scanner, and the system time was written into the list-mode scan data. The median speed of motion of the moving line

source was 6.3 mm/sec, which is much higher than the median speed of motion of the NHP head to stress the motion correction and the time synchronization algorithms. The rod source data were reconstructed without attenuation or scatter correction. The contrast recovery coefficient (CRC), here defined as (Hot-Cold)/Hot, was used to examine the image resolution and the effect of residual intra-frame motion.

Supplemental Fig. 3 shows the effect of time synchronization between list-mode data and motion data in a rotating rod source study. All images are displayed in the transaxial view. Supplemental Figs. 3B, C, D, F, G and H are displayed on a common scale, and Supplemental Figs. 3A and E are displayed to a different scale to better visualize the effect of motion. The top row shows the images reconstructed with FBP (Ramp filter at Nyquist frequency) for a rotating rod scan without motion correction (Supplemental Fig. 3A), with MAF motion correction but *without* time synchronization (Supplemental Fig. 3B), with MAF motion correction and with time synchronization (Supplemental Fig. 3C), and a static rod scan (Supplemental Fig. 3D). Each subframe has an IFMT of 2 mm and MFDT of 3 sec, which keeps 32% of the scan data. The bottom row shows the images reconstructed with MOLAR for a rotating rod scan without motion correction (Supplemental Fig. 3E), with event-by-event (EBE) motion correction but *without* time synchronization (Supplemental Fig. 3F), with EBE motion correction and with time synchronization (Supplemental Fig. 3G), and a static rod scan (Supplemental Fig. 3H).

Compared with the images reconstructed without motion correction (Supplemental Figs. 3A and 3E), both the MAF (Supplemental Figs. 3B and 3C) and the EBE (Supplemental Figs. 3F and 3G) motion correction methods corrected most of the motion. Without time synchronization, noticeable image artifacts are observed in Supplemental Fig. 3F as compared with Supplemental Fig. 3G, suggesting that precise time synchronization is necessary in EBE motion correction. The effect of time synchronization is less obvious for the MAF motion correction method, as Supplemental Fig. 3B shows less blurring than Supplemental Fig. 3F since large motions were

excluded. The degradation in image resolution for the motion corrected images (Supplemental Figs. 3C and 3G) compared to the static studies (Supplemental Figs. 3D and 3H) is likely due to the uncertainty in the motion data.



Supplemental Fig. 3. Rotating rod source study showing the effect of time synchronization between motion tracking and scanner computers. The top row shows the images reconstructed with FBP for a rotating rod scan without motion correction (A), with MAF motion correction but *without* time synchronization (B), with MAF motion correction and with time synchronization (C), and a static rod scan (D). Each subframe has an intra-frame motion threshold (IFMT) of 2 mm and a minimum frame duration threshold (MFDT) of 3 sec, which keeps 32% of the scan data. The bottom row shows the images reconstructed with MOLAR for a rotating rod scan without motion correction (E), with EBE motion correction but *without* time synchronization (F), with EBE motion correction and with time synchronization (G), and a static rod scan (H). Time synchronization is necessary to enhance the accuracy of motion data, especially for the EBE motion correction method. B, C, D, F, G and H are displayed on a common scale, and A and E are displayed to a different scale to better visualize the effect of motion.

It is worth noting that accurate time synchronization between the motion data and the scan data is more important for EBE motion than MAF motion correction, as we observed more blurring effects in EBE motion correction (Supplemental Fig. 3F) than MAF motion correction (Supplemental Fig. 3B) if no time synchronization was applied. This is because the mismatch in time between the motion data and the scan data has substantial effects in resolution degradation when the speed of motion is large. However, scan data are discarded when rapid motion within short intervals occurs for MAF, thus reducing the effect of inaccurate time information in the motion data. On the contrary, EBE motion correction uses all the events, and is thus more affected by any temporal uncertainty in the motion data. Therefore, accurate time synchronization between the motion and scan data is critical for EBE motion correction.

Scanner setup in the awake NHP studies



Supplemental Fig. 4. MicroPET scanner FOCUS-220 raised and tilted forward $\sim 45^\circ$ with a lifter-tilter. The Vicra camera was hung on the ceiling and positioned towards the bore of the scanner.